

Material Mechanics Research

C.T. Liu

February 2003

Final Report

APPROVED FOR PUBLIC RELEASE; DISTRIBUTION UNLIMITED.



**AIR FORCE RESEARCH LABORATORY
AIR FORCE MATERIEL COMMAND
EDWARDS AIR FORCE BASE CA 93524-7048**

REPORT DOCUMENTATION PAGEForm Approved
OMB No. 0704-0188

Public reporting burden for this collection of information is estimated to average 1 hour per response, including the time for reviewing instructions, searching existing data sources, gathering and maintaining the data needed, and completing and reviewing this collection of information. Send comments regarding this burden estimate or any other aspect of this collection of information, including suggestions for reducing this burden to Department of Defense, Washington Headquarters Services, Directorate for Information Operations and Reports (0704-0188), 1215 Jefferson Davis Highway, Suite 1204, Arlington, VA 22202-4302. Respondents should be aware that notwithstanding any other provision of law, no person shall be subject to any penalty for failing to comply with a collection of information if it does not display a currently valid OMB control number. **PLEASE DO NOT RETURN YOUR FORM TO THE ABOVE ADDRESS.**

1. REPORT DATE (DD-MM-YYYY) 01-12-2002		2. REPORT TYPE Final		3. DATES COVERED (From - To) 15 Dec 1987 – 30 Sep 2002	
4. TITLE AND SUBTITLE Material Mechanics Research				5a. CONTRACT NUMBER	
				5b. GRANT NUMBER	
				5c. PROGRAM ELEMENT NUMBER 61102F	
6. AUTHOR(S) C. T. Liu				5d. PROJECT NUMBER 2302	
				5e. TASK NUMBER M1G2	
				5f. WORK UNIT NUMBER 346120	
7. PERFORMING ORGANIZATION NAME(S) AND ADDRESS(ES) Air Force Research Laboratory (AFMC) AFRL/PRSM 10 E. Saturn Blvd. Edwards AFB CA 93524-7680				8. PERFORMING ORGANIZATION REPORT NO. AFRL-PR-ED-TR-2003-0006	
9. SPONSORING / MONITORING AGENCY NAME(S) AND ADDRESS(ES) Air Force Research Laboratory (AFMC) AFRL/PRSM 10 E. Saturn Blvd. Edwards AFB CA 93524-7680				10. SPONSOR/MONITOR'S ACRONYM(S)	
				11. SPONSOR/MONITOR'S REPORT NUMBER(S) AFRL-PR-ED-TR-2003-0006	
12. DISTRIBUTION / AVAILABILITY STATEMENT Approved for public release; distribution unlimited; February 2003.					
13. SUPPLEMENTARY NOTES					
14. ABSTRACT This report covers results of research addressing cumulative damage and crack growth behavior in a solid propellant and interfacial fracture of bi-material bonded systems. The program's basic approach involves a blend of analytical and experimental studies. In general, mechanisms and mechanics involved in cohesive fracture in the solid propellant and adhesive fracture in the bi-material bonded systems are emphasized. The results of both analytical and experimental analyses are evaluated and discussed.					
15. SUBJECT TERMS rocket; propellant; damage; crack growth; bi-material; bonded systems					
16. SECURITY CLASSIFICATION OF:			17. LIMITATION OF ABSTRACT A	18. NUMBER OF PAGES	19a. NAME OF RESPONSIBLE PERSON C. T. Liu
a. REPORT Unclassified	b. ABSTRACT Unclassified	c. THIS PAGE Unclassified			19b. TELEPHONE NO (include area code) (661) 275-5642

Standard Form 298
(Rev. 8-98)
Prescribed by ANSI Std. Z39.18

NOTICE

When U.S. Government drawings, specifications, or other data are used for any purpose other than a definitely related Government procurement operation, the fact that the Government may have formulated, furnished, or in any way supplied the said drawings, specifications, or other data, is not to be regarded by implication or otherwise, or in any way licensing the holder or any other person or corporation, or conveying any rights or permission to manufacture, use or sell any patented invention that may be related thereto.

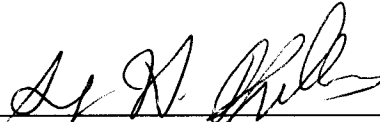
FOREWORD

This final technical report, entitled "Material Mechanic Research," presents the results of an in-house study performed under JON 2302M1G2 by AFRL/PRSM, Edwards AFB CA. The Principal Investigator/Project Manager for the Air Force Research Laboratory was Dr. C.T. Liu

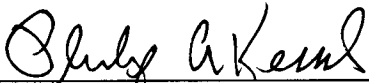
This report has been reviewed and is approved for release and distribution in accordance with the distribution statement on the cover and on the SF Form 298.



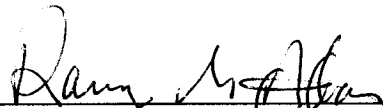
C.T. Liu
Project Manager



SHAWN H. PHILLIPS
Chief
Propulsion Materials Application Branch



PHILIP A. KESSEL
Technical Advisor
Space & Missile Propulsion Division



RANNEY G. ADAMS III
Director
Public Affairs
AFRL PAS 03-064 (GRS)

TABLE OF CONTENTS

INTRODUCTION -----	1
OBJECTIVES -----	1
TASK 1 – INVESTIGATING THE EFFECTS OF PRESSURE, STRAIN RATE, AND DAMAGE ON CRACK GROWTH BEHAVIOR IN A SOLID PROPELLANT -----	1
TASK 2 – CRACK INSTABILITY AND GROWTH MODELS -----	3
TASK 3 – PHOTOELASTIC ANALYSIS OF THREE-DIMENSIONAL EFFECTS OF CRACKING OF MOTOR GRAIN GEOMETRIES UNDER INTERNAL PRESSURE LOADS -----	6
TASK 4 – DEFORMATION AND FRACTURE OF BONDED SYSTEMS -----	7
REFERENCES -----	8

GLOSSARY

psi	pounds per square inch
RL	Ravi-Lin
SFI	stress intensity factor
Tc	coefficient of thermal expansion
μ_0	undamaged material shear modulus
τ	relaxation time
κ_0	undamaged material bulk modulus

Introduction:

The goal of this program is to develop a basis for developing advanced crack growth and service life prediction technologies for predicting the service life of solid rocket motors. The objectives of this program are to : (1) gain a fundamental understanding of fracture and crack growth behavior in solid rocket motors; (2) investigate the effects of damage, material nonlinearity, pressure, and loading rate on crack growth behavior in a solid propellant; (3) simulate crack growth behavior and gain insight for improving crack growth resistance in solid propellants; and (4) determine the strain rate effect on the constitutive and fracture behavior of bi-material bond systems. The main issues in service life prediction of solid rocket motors are the lack of a fundamental understanding of crack growth behavior under service loading conditions and a reliable methodology to predict crack growth. The main technical challenges are microstructural effects on damage initiation and evolution, large and time dependent deformation, short crack and stress raiser interaction, and multi-layer structures with time-dependent material properties and property gradients. The program's basic approach involves a blend of analytical and experimental studies. In general, mechanisms and mechanics involved in cohesive fracture in a solid propellant and adhesive fracture in bond systems are emphasized. In this program, nonlinear viscoelasticity, fracture mechanics, experimental mechanics, damage mechanics, nondestructive testing and evaluation, and numerical modeling techniques will be used.

Objectives:

These research studies address a number of important subjects. There are four major tasks: (1) Task 1- investigating the effects of pressure, strain rate, and damage on crack growth behavior in a solid propellant, (2) Task 2 – developing a failure envelope to predict the critical stress for the onset of growth of short cracks, (3) Task 3 – investigating the three-dimensional effect on crack growth behavior, and (4) Task 4 - determining the strain rate effects on the constitutive behavior as well as on the local damage and deformation in bi-material, propellant/liner/propellant, bond systems. The results of these studies have the potential of becoming some of the most significant contributions to the rocket industry and research community.

Summary of Accomplishments:

Task 1: Investigating the Effects of Pressure, Strain Rate, and Damage on Crack growth Behavior in a Solid Propellant

In Task 1, experiments were conducted on uniaxial specimen with two different initial crack lengths (0.1 in. and 0.3 in.) at four different displacement rates (0.2 in/min, 2 in/min, 50 in/min, and 200 in/min) under three confined pressures (ambient, 500 psi, and 1000 psi). Experimental findings reveal that cracks grow slower under confined pressure. The decrease in crack growth rate under confined pressure is due to the suppression of the development of damage in the material and the decrease in strain gradient near the crack tip (1-6). The experimental findings also reveal that, after the crack propagates, the growth behavior of the two initial crack lengths considered are similar.

REPORT DOCUMENTATION PAGE

Form Approved OMB No.
0704-0188

Public reporting burden for this collection of information is estimated to average 1 hour per response, including the time for reviewing instructions, searching existing data sources, gathering and maintaining the data needed, and completing and reviewing this collection of information. Send comments regarding this burden estimate or any other aspect of this collection of information, including suggestions for reducing this burden to Department of Defense, Washington Headquarters Services, Directorate for Information Operations and Reports (0704-0188), 1215 Jefferson Davis Highway, Suite 1204, Arlington, VA 22202-4302. Respondents should be aware that notwithstanding any other provision of law, no person shall be subject to any penalty for failing to comply with a collection of information if it does not display a currently valid OMB control number. PLEASE DO NOT RETURN YOUR FORM TO THE ABOVE ADDRESS.

1. REPORT DATE (DD-MM-YYYY) 01-12-2002	2. REPORT TYPE Final	3. DATES COVERED (FROM - TO) 15-12-1995 to 30-12-2002
--	--------------------------------	---

4. TITLE AND SUBTITLE Material Mechanics Research Unclassified	5a. CONTRACT NUMBER
	5b. GRANT NUMBER
	5c. PROGRAM ELEMENT NUMBER 61102F

6. AUTHOR(S) Liu, C. T. ;	5d. PROJECT NUMBER 2302
	5e. TASK NUMBER M1G2
	5f. WORK UNIT NUMBER

7. PERFORMING ORGANIZATION NAME AND ADDRESS Air Force Research Laboratory (AFMC) AFRL/PRSM 10 E. Saturn Blvd. Edwards AFB, CA93524-7680	8. PERFORMING ORGANIZATION REPORT NUMBER AFRL-PR-ED-TR-2003-0006
--	--

9. SPONSORING/MONITORING AGENCY NAME AND ADDRESS Air Force Research Laboratory (AFMC) AFRL/PRSM 10 E. Saturn Blvd. Edwards AFB, CA93524-7680	10. SPONSOR/MONITOR'S ACRONYM(S)
	11. SPONSOR/MONITOR'S REPORT NUMBER(S) AFRL-PR-ED-TR-2003-0006

12. DISTRIBUTION/AVAILABILITY STATEMENT
A PUBLIC RELEASE

13. SUPPLEMENTARY NOTES
Actual dates covered (block 3) are: 15 Dec 1987 - 30 Sep 2002.

14. ABSTRACT
This report covers results of research addressing cumulative damage and crack growth behavior in a solid propellant and interfacial fracture of bi-material bonded systems. The program's basic approach involves a blend of analytical and experimental studies. In general, mechanisms and mechanics involved in cohesive fracture in the solid propellant and adhesive fracture in the bi-material bonded systems are emphasized. The results of both analytical and experimental analyses are evaluated and discussed.

15. SUBJECT TERMS
rocket; propellant; damage; crack growth; bi-material; bonded systems

16. SECURITY CLASSIFICATION OF:	17. LIMITATION OF ABSTRACT Public Release	18. NUMBER OF PAGES 17	19. NAME OF RESPONSIBLE PERSON Liu, C.T. Chi.Liu@edwards.af.mil
--	---	----------------------------------	--

<table style="width: 100%; border-collapse: collapse;"> <tr> <td style="width: 33%; padding: 2px;">a. REPORT Unclassified</td> <td style="width: 33%; padding: 2px;">b. ABSTRACT Unclassified</td> <td style="width: 33%; padding: 2px;">c. THIS PAGE Unclassified</td> </tr> </table>	a. REPORT Unclassified	b. ABSTRACT Unclassified	c. THIS PAGE Unclassified	19b. TELEPHONE NUMBER International Area Code Area Code Telephone Number 661275-5642 DSN 525-5642
a. REPORT Unclassified	b. ABSTRACT Unclassified	c. THIS PAGE Unclassified		

In addition to conducting the experiments, the focus of research also centered on the effect of hydrostatic pressure on damage and the constitutive behavior of the material. Particularly, the study was conducted on modeling the effect of hydrostatic pressure on the progressive damage. A multi-scale approach was used along with a damage theory at the matrix material level. The multi-scale approach is based on the interconnection between the microlevel (i.e., particle and matrix material level) and the macrolevel (i.e., the particulate composite level). In order to model the effect of hydrostatic pressure on the damage, the damage theory previously developed was modified.

It has been shown that the damage function for solid propellants could be well expressed in terms of the total strain energy density. The strain energy has two parts: dilatational energy and distortional energy. While increasing distortional energy contributes to the damage, dilatational energy needs to be treated properly depending on positive and negative dilatation. If dilatation is positive, it is added to the distortional energy because it also causes damage. However, negative dilatation is not added to the distortional energy because it does not produce damage. Consequently, the strain energy damage function is expressed as :

$$f = u_d + H(e)u_v \quad (1)$$

where u_d and u_v are distortional and dilatational energy density, and H is the Heaviside unit step function defined such that $H(e) = 1$ when $e > 0$ and $H(e) = 0$ when $e < 0$. The parameter e denotes dilatation. Thus, hydrostatic pressure (negative dilatation) affects damage initiation and growth. The predicted stress-strain curves under hydrostatic pressure of 0 and 1000 psi, respectively, are plotted and compared to the experimental curves. The comparison is excellent so that the damage function of Equation (1) was proved to be valid.

The developed time-independent constitutive model was incorporated in a computer code, which was used to predict the initial crack length in high stress regions in an analogy specimen under a multi-axial loading condition (7-10). The results are discussed in the following paragraphs.

Damage growth and crack initiation at a notch with stress concentration was studied using an analog specimen. For the analog specimen, there are two different notch radii, one large and one small. Therefore, there are two stress concentration locations in the specimen which are consistent with the results obtained from a photoelastic analysis. In the finite element analysis, 3-D solid elements with eight nodes per element were used. In the numerical analysis, a uniform displacement was applied to the slanted top boundary of the specimen and the symmetric boundary conditions were applied to the horizontal bottom boundary.

The notched specimen under tensile load with the displacement control was first studied without hydrostatic pressure. Before damage began in the specimen, the stress in the loading direction was the greatest at the element that was located at the intersection between the large and small radii of the notch. This element is called the 'small radius element' in the following discussion. Consequently, damage started to form at this site first. However, the stress level at the element on the symmetric boundary was quite comparable to that of the small radius element so that damage

followed subsequently on the symmetric boundary. The element on the symmetric boundary is called the 'large radius element' from now on. Eventually, damage saturated at the small radius element and the initial crack size, using the criterion discussed previously, was 1.7 mm long. The experimentally measured crack length was 1.86 mm in average so that there was a good agreement between the predicted and measured initial crack lengths.

The same kind of specimen was subjected to hydrostatic pressure of 1000 psi and also loaded in tension with the displacement control. For this case, the stress along the loading direction was the largest at the small radius element with initial damage. The large radius element competed with the small radius element in damage growth and the former had the damage saturation earlier than the latter. The initial crack size was 1.7 mm at section of the large radius element.

Task 2: Crack Instability and Growth Models

Sub-Task 1: Instability Criteria for Short Crack Growth

In this task, the instability criteria for the onset of growth of short cracks are developed. Based on experimental findings, we find that for short cracks, defined as having a crack length equal to or less than 0.1 in., classic fracture mechanics cannot be used to determine the critical condition for the onset of crack growth. In order to predict the onset of growth of short cracks, a linear fracture mechanics solution was modified to predict the behavior of short cracks. An effective crack length, which was equal to the original crack length plus the length of the failure process zone, was introduced into the Mode I stress intensity factor. By using the effective crack length, a reasonably good agreement exists between the fracture toughnesses for the onset of growth of short and long cracks. In addition, a failure envelope, based on theories of strength of material and fracture mechanics, was also developed. The developed failure envelope can be used to predict the critical stress for the onset of crack growth for short and long cracks under different strain rate and confining pressure conditions.

Sub-Task2: Determining the Damage Characteristics near the Crack Tip

In this task, Lockheed-Martin Research Laboratory's High-Resolution Digital Real-Time Radiographic System and acoustic imaging systems were used to determine the damage characteristics near the crack tip for different materials (11-13). The experimental results reveal that the critical damage intensity for the onset of crack growth is insensitive to loading history and material property. However, due to the viscoelastic nature of the materials, load history and time have a significant effect on the damage characteristics in the materials. Therefore, caution should be exercised when interpreting the nondestructive testing results.

Sub-Task 3: Predicting the Critical Inherent Initial Crack Length in the Material

In this task, a technique was developed (14), based on fracture mechanics and probabilistic mechanics, to predict the critical inherent initial crack size. The developed technique can be used

to predict the critical inherent initial crack size at different strain rates with good accuracy (15). For example, at 18.182 in./in./min strain rate, the predicted and the measured initial critical crack sizes are 0.146 in. and 0.132 in., respectively. The results also show that the critical inherent initial crack sizes are insensitive to strain rate. For example, at 0.067 in./in./min and 0.727 in./in./min strain rates the predicted critical inherent initial crack sizes are 0.13 in. and 0.119 in., respectively. In addition, the strain rate has no significant effect of the statistical distribution function of the critical inherent initial crack length. For the three strain rates considered, the statistical distribution functions of the critical inherent initial crack length follow the Second Asymptotic Distribution of the Maximum Value.

In addition, the results of the analysis reveal that the magnitudes of the confining pressure, ambient and 1000 psi, have no significant effect on the predicted critical initial crack length. It also reveals that the critical initial crack length and the statistical distribution function are insensitive to specimen's thickness, strain rate, and loading axially. Therefore, for the material investigated, the critical initial crack length can be considered a material property. The determination of the critical initial crack size and its statistical distribution function will make statistical and reliability analyses of crack growth feasible.

Sub-Task 4 Numerical Simulation of Crack Growth

In order to develop a fundamental understanding of the crack growth process, the crack-tip fields obtained from the numerical simulations were examined. The numerical simulation results suggest that the crack growth occurs in a discrete manner and upon the attainment of a critical state of strain at a critical distance ahead of the crack tip. This is consistent with the critical damage criterion that is used in the simulations.

In this sub-task, crack propagation at room temperature in a solid propellant was analyzed at different loading rates using a modified Ravi-Liu (RL) model by including time dependence of the homogenized material, i.e., particulate composite with a rubbery matrix and high stiffness particles. Experimental observations show that the volume dilatation Θ (damage parameter in RL model) (16) is independent of the loading rate and is purely a function of applied strain. In other words, volume dilatation is dependent only on mechanical deformation (strain). Taking these observations into account, the material time dependence is introduced through a simple Maxwell model for the undamaged material, and it is assumed that both the bulk and shear response of the material are governed by the same relaxation time, τ . The undamaged material's bulk (κ_o) and shear (μ_o) moduli are given in terms of its rubbery moduli, κ_∞ and μ_∞ and Prony coefficients κ_1 and μ_1 ,

$$\kappa_o(t) = \kappa_\infty + \kappa_1 \exp(-t/\tau) \quad \text{and} \quad \mu_o(t) = \mu_\infty + \mu_1 \exp(-t/\tau). \quad (2)$$

Stress components σ_{ij} are evaluated using the convolution integral,

$$\mathbf{s}_{ij}(t) = \int_0^t \mathbf{k}_o(t-t')g(\Theta)\mathbf{d}_{ij}dt' + \int_0^t 2\mathbf{m}_o(t-t')h(\Theta)\mathbf{e}_{ij}dt' \quad (3)$$

where g and h are the damage parameters, which are purely functions of the volume dilatation.

The modified viscoelastic RL model has been implemented in a special purpose displacement based finite element code, FEAP-SP. The damage parameters governing the degradation of the bulk and the shear moduli, g and h are determined using the uniaxial response and dilatation data as outlined in the original RL model. The finite element method uses the Newton-Raphson iterative procedure for achieving force equilibrium and Newton's iterative method for enforcing a plane stress condition. Constitutive update (stress, dilatation) is performed through integration of Equation (2) for a finite time step. Time steps are chosen to preserve accuracy in the constitutive update and to ensure quadratic convergence of the residual energy norm.

Crack propagation was simulated in specimens with edge cracks subjected to prescribed displacement rates at the boundaries. Due to the inherent nature of the singular stress fields near the crack tip, the loading rate varies by at least two orders of magnitude from the loading boundary to the crack tip. The relaxation and damage parameters determined from the uniaxial stress-strain curves are used in the finite element calculations to update the local moduli as well as damage. Crack initiation and propagation is performed using a node release technique. Attainment of critical dilatation is used as the crack initiation criteria. The FE model continues to check at the end of every time step elements that have attained the specified critical dilatation. Once the critical dilatation is reached in an element (usually at the crack tip), the reaction force is computed at the crack tip node. Then the computed nodal force replaces the crack tip displacement specified condition. Now, holding the far field displacement fixed at the time of crack initiation, the nodal force at the crack tip is relaxed over a specified number of steps (typically 20). At the end of this node release procedure, the crack is deemed to propagate across the element in which critical dilatation had been reached. The time taken to relax the nodal force is kept to a minimum, typically 0.1% of the time step, so as not to artificially relax the material properties. Once the node release has been accomplished, i.e., the nodal force reaching zero, the corresponding boundary condition for that node is changed to traction free. Then, the far field loading is continued as before until the critical dilatation is reached in an element and then the previously mentioned node release procedure is repeated. Hence, crack propagation in the finite element calculations is a discrete process and from the times at which the critical dilatation is reached at the crack tip positions, change in crack length as a function of time can be computed. At every load step, the reaction force is computed which would provide the boundary load as a function of time. Once the node release becomes untenable, i.e., attaining critical conditions in one or more elements without sustaining further loading, the crack propagation is said to be unstable and the computations are terminated.

Simulations of crack growth were carried out in a solid propellant at two different rates, 0.1 in/min and 0.5 in/min and room temperature (17)). Displacements were specified at the specimen boundaries normal to the crack. The load increases nearly linearly with increasing displacement with the crack blunting monotonically. Upon reaching the critical dilatation in the crack tip vicinity, crack growth is initiated. The initiation time is in fairly good agreement with experimentally measured values. Upon initiation, the load gradually level off and agrees closely with experimental observations. Upon crack initiation, the successive elements near the crack tip

fail and node release is used to propagate the crack. The crack exhibits blunting-sharpening-blunting sequence during crack growth indicating the discontinuous nature of crack propagation in solid propellants. The crack growth data from the numerical simulations indicate that the predictions show a similar trend for the experiments with higher crack propagation velocities. Crack tip fields have also been examined which show self-similarity in damage patterns (e.g., dilatation) during crack growth. These simulations have validated, for the first time, an approach for realistic modeling of crack growth and hence prediction of crack length as function of time and loading rates in solid rocket motors. Such a simulation capability could be a useful tool in predicting life of rocket motors in service.

Task 3: Photoelastic Analysis of Three-Dimensional Effects of Cracking of Motor Grain Geometries under Internal Pressure Loads

In order to obtain some insight into the three-dimensional effects of cracking of motor grain geometries under load, a series of experiments on photoelastic scale models of motor grain were conducted using the frozen stress method. The models were capped at the ends and pressurized internally above critical temperature after real cracks were introduced at fin tips in critical locations. After growing to desired size, pressure was reduced to stop growth and held through cooling.

Photoelastic analysis of the selected model geometry (18-19) show that there are two critical locations at a fin tip; one at the confluence of the edge radius of $R = 1.3$ mm with the radius $R = 11.0$ mm of the central part of the fin tip, and the other on the fin axis itself. There are two positions on each fin tip where the confluence of the two above noted radii exist. A crack emanating from such a position we call an off-axis crack. A crack at the other location on a fin axis we call a symmetric crack, which, in this case, is symmetric with respect to both load and geometry, and is a Class I crack which grows readily. Off-axis cracks, however, generally do not occupy principal planes of stress or planes of symmetry, and are generally called Class II cracks which must turn or kink to eliminate some Mode II before becoming purely Mode I at which time they will grow readily as Class I cracks. By placing both types of cracks in the same model separated by uncracked or plugged fins, (plugs are cylinders used to seal holes made to allow the insertion of a shaft which carries a blade to a critical locus at the fin tip), it is confirmed that the symmetric cracks penetrate to the outer surface of the model before the off-axis cracks have grown significantly. Data also reveal that a shear mode along with Mode I in the off-axis cracks before they are completely turned.

Experimental findings reveal that the turning effect in three dimensional off-axis cracks involves a shear mode except near the fin tip surface and, in non-brittle materials, turns rather than kinks sharply. Upon eliminating the shear mode, pure Mode I occurs all along the crack front in the Class I sense. It also reveals that cracks symmetric in both load and geometry will grow far more readily than off-axis cracks due to the shear mode effect in the latter even though the stress maybe higher at the off-axis locus in an uncracked fin.

If the above observations are projected to motor grain, then at sufficiently low temperatures, which stiffen the matrix to the level of the hard particles, the above-described behavior might occur. However, at higher temperatures, large microscopic shear mode effects would likely occur, during particulate rearrangement and dewetting, probably retarding crack growth.

Taken collectively, the above studies suggest the following observations: (1) Symmetric cracks are more dangerous than off-axis cracks even though they do not start at the locus of maximum stress in the uncracked model. (2) Off-axis cracks directed parallel to the fin axis are also dangerous but less so than the symmetric cracks for they will grow on slightly curved, and (3) While some of the cracks penetrated the outer wall in the depth direction, none of the cracks penetrated the length of the cylinder.

These results suggest that the practice of using a through-the-cylinder length crack in design maybe a substantial over design and suggests a comparison with deep semi-elliptic cracks as an alternative approach.

Task 4: Deformation and Fracture of Bonded Systems

Sub-Task 1: Determining the Stress Intensity Factors for Interfacial Cracks in Bi-Material Bonded Systems

The objectives of this study were to determine the three dimensional and residual stress effects on the distribution of the stress intensity factor (SIF) K_I along the interfacial cracks in bi-material specimens. In this task, both stress frozen and photoelastic techniques were used to determine the SIF along the interfacial cracks, through and part-through cracks, in bi-material specimens using a three-specimen test method. A three specimens test series was conducted for each crack depth involving (1) A homogeneous edge cracked specimen, (2) a homogeneous bonded edge cracked specimen, and (3) An edged cracked bimaterial specimen (19-22). After no load and fully loaded stress freezing cycles, slices were removed along the crack front. The results reveal that there is little variation, within experimental scatter, between the side slices and the center slice but center slice results are always higher so only center slice results are reported.

Experimental data indicate that the fringes are continuous across the upper bondline since the adhesive is chemically the same as the upper material. However, there is a disturbance along the lower bondline where the material mismatch occurs. This pattern contrasts from the results for through cracks. This led to significantly different values of K_I above and below the bondline for the part through crack. In order to determine which (if either) values of K_I was correct in this case, a separate experiment was performed on a model consisting of materials where there is no T_c mismatch and which had previously been found to yield good results for through cracked specimens. In the analysis, the K_I values on both sides of the crack were averaged. While no clear technical explanation can be made to support this step to correct asymmetry apparently due to T_c mismatch and perhaps other effects, nevertheless the test with no T_c mismatch mentioned above, showed reasonable agreement for this procedure.

Finally, when comparing results of the part through cracks with those for through cracks by matching a/t for the part through crack with a/w of the through crack at 0.25, the through crack yielded higher SIF values in the ratio of $1.82/1.21 = 1.50$ suggesting that the part through cracks are much less severe as expected.

Sub-Task 2 Deformation and Failure Mechanism of Propellant/Liner/Propellant Bonded Specimens

In this task, a series of experiments on propellant/liner/propellant bonded specimens were conducted at 0.01 in/min displacement rate. A computer aided speckle interferometry technique was used to determine the displacement and strain distributions in the specimen. Two interface debonding modes, debonding from the center and the corner of the interface of the specimen, are observed. These debonding modes appear to be related to the specimen geometry. In addition, the strain rates in the interphase and liner layers increase with increasing time, which are significant different from the constant applied strain rate (23).

References

- (1) Liu, C. T., "Investigating the Effects of Specimen Thickness and Pressure on the Crack Growth Behavior of a Particulate Composite Material," *The 14th U.S. National Congress of Theoretical and Applied Mechanics* (invited paper), June 2002.
- (2) Miller, T. C. and Liu, C. T., "The Effects of Pressure on Fracture of a Rubbery Particulate Composite," *Society for Experimental Mechanics IX International Congress and Exposition, Orlando, Florida 2000*.
- (3) Liu, C. T. and Smith, C. W., "Near Tip Behavior in a Particulate Composite Material under Constant Strain Rate Including Temperature and Thickness Effects," *International Conf. on Fracture, Dec. 2001*.
- (4) Liu, C. T., "Strain Rate Effect on Crack Opening and Growth in a Particulate Composite Material at Low Temperature," *3rd International Conf. Mechanics of Time Dependent Material*, 18-20 Sept. 2000, Erlangen Germany.
- (5) Yen, M. and Liu, C. T., "Effect of Strain Rate on the Near Crack Tip Behavior of a Particulate Composite," *International Journal of Damage Mechanics*, Vol.9 Oct. 2000.

- (6) Liu, C. T. and Miller, T. C., "Effect of Crack Size on Initiation of Propagation and Growth Behavior in a Particulate Composite Material," *SEM IX International Congress on Experimental mechanics*, Orlando, FL. 5-8 June, 2000.
- (7) Kwon, Y.W. and Liu, C. T., "Numerical Study of Damage Growth in Particulate Composites", Transactions of ASME: *Journal of Engineering Materials and Technology*, Vol. **121**, Oct. 1999.
- (8) Kwon, Y. W. and Liu, C. T., "Prediction of Initial Crack Size in Particulate Composites with a Circular Hole", *Mechanics Research Communications*, Vol. **27**, No. 4, 2000.
- (9) Kwon, Y. W. and Liu, C. T., "Modeling of Hydrostatic Pressure Effect on Progressive Damage in Particulate Composites", *Recent Advances in Solids and Structures -2000*, ASME, 2000.
- (10) Kwon, Y.W. and Liu, C. T., "Effect of Particle Distribution on Initial Cracks Forming from Notch Tips of Composites with Hard Particles Embedded in a Soft Matrix", *Composites, Part B: Engineering*, Vol. **32**, 2001.
- (11) Liu, C. T., "Observation of Damage Process in a Particulate Composite Material using Real-Time X-Ray Techniques," *Journal of Nondestructive Testing and Evaluation* Vol.**17** Number 3 2001.
- (12) Liu, C. T., "Monitoring Damage Initiation and Evolution in a Field Polymeric Material Using Nondestructive Testing Techniques," *Composites and Structures* **76**, 2000.
- (13) Liu, C. T., "Effect of Load History on Damage Characteristics near Crack Tips in a Particulate Composite Material," *Internal Journal of Damage Mechanics*, Vol. **9**-Jan 2000.
- (14) Liu, C. T. and Yang, J. N. (Invited Paper), "Determination of Equivalent Initial Flaw Size in a Particulate Composite Material," *8th ASCE Conf. on Probabilistic Mechanics and Structural Reliability*, Notre Dame, IN. 24-26 July, 2000.
- (15) Liu, C. T. and Yang, J. N., "Investigating the Effect of Strain Rate on the Equivalent Initial Crack Size in a Particulate Composite Material," *The Fourth International Conf. on Computational Stochastic Mechanics*, June 2001
- (16) Liu, C. T. and Ravichandran, G., " An Experimental and Numerical Analysis of Near Tip Behavior in a Mult-Phase Material." *1997 ASME Winter Meeting*, Nov. 1997.
- (17) Burcsu, E. and Ravichandran, G., " Crack Initiation and Growth in Viscoelastic Particulate Composites." *SEM IX International Congress & Exposition on Experimental Mechanics*, June, 2000.

- (18) Smith, C. W., Constantinescu, D. M., and Liu, C. T., “Stress Intensity Factors and Paths for Cracks in Photoelastic Motor Grain Models Under Internal Pressure,” *Recent Advances in Solids and Structures-2001*, ASME PVP Vol. **520**, 2001.
- (19) Smith, C. W., Constantinescu, D. M., and Liu, C. T., “SIF distributions in Cracked Photoelastic Rocket Motor models; Preliminary Studies,” *SEM Annual Conf. on Experimental and Applied Mechanics*, June, 2001.
- (20) Smith, C. W., Gloss, K. T., and Liu, C. T., “Test Geometries for Bondline Cracked Photoelastic Models: Preliminary Results,” *Recent Advances in Solid and Structures*, ASME-PVP Vol. **398** Nov.1999.
- (21) Smith, C. W., Finlayson, E. F., and Liu, C. T., “Stress Intensity Factors in Part Through Bondline Cracks in Incompressible Materials,” *SEM Annual Conf. on Experimental Mechanics*, June, 1999.
- (22) Smith, C. W. and Liu, C. T., “Effect of Material Properties on Stress Intensity Factor Measurement by the Frozen Stress Method,” *1999 ASME International Engineering Conf on Polymeric Systems*, MD Vol. **88**, 1999.
- (23) Liu, C. T. and Fu-Pen Chiang, “Investigating the Deformation and failure Mechanisms in a Bi-Material Systems Under Tension,” *Proceeding of The 14th U.S. National Congress of Theoretical and Applied Mechanics*, June, 2002.

AFRL-PR-ED-TR-2003-0006
Primary Distribution of this Report:

AFRL/PRSM (10 CD + 10 HC)
C.R. Liu
10 E. Saturn Blvd.
Edwards AFB CA 93524-7680

Naval Surface Warfare Center (1 CD + 1 HC)
Frank C. Tse
Code 4OP1 (Tech Library)
101 Strauss Ave.
Indian Head, MD 20640-5035

Joe Chamlee (1 CD + 1 HC)
Tech Library
Code ED22/Bldg 4666
Marshall Space Flight Center, AL 35812-0000

AFRL/PR Technical Library (2 CD + 1 HC)
6 Draco Drive
Edwards AFB CA 93524-7130

Chemical Propulsion Information Agency (1 CD)
Attn: Tech Lib (Dottie Becker)
10630 Little Patuxent Parkway, Suite 202
Columbia MD 21044-3200

Defense Technical Information Center
(1 Electronic Submission via STINT)
Attn: DTIC-ACQS (Acquisitions)
8725 John J. Kingman Road, Suite 94
Ft. Belvoir VA 22060-6218

Dr. Robert R. Little (1 CD + 1 HC)
US Army Aviation and Missile Command
AMSAM-RD-PS-S (Tech Library)
Redstone Arsenal, AL 35898

Naval Air Warfare Center, Weapons Division
Robert W. Pritchard (1 CD + 1HC)
1 Administration Circle
China Lake, CA 93555-6100

AFRL/PROI (1 CD + 1 HC)
Ranney G. Adams
2 Draco Drive
Edwards AFB, CA 93524

NASA/AMES
James P. Hawkins (1 CD + 1 HC)
ED22 Strength Analysis Group
Marshall Space Flight Center, AL 35812

NASA Marshall Space Flight Center
David W. Ricks (1 CD + 1 HC)
Bldg 4202/Room 507
Marshall Space Flight Center, AL 35812

AFRL/PRSB
Gregory A. Ruderman (1 CD + 1 HC)
4 Draco Drive
Edwards AFB, CA 93524-7160

Aerojet
Richard K. McCamey (1 CD + 1 HC)
B-05025/D-5263
P.O. Box 13222
Sacramento, CA 95813-1600

Thiokol Corporation
Robert P. Graham (1 CD + 1HC)
MS-252
P.O. Box 707
Brigham City, UT 84302-0707

AMCOM
Robert N. Evans (1 CD + 1 HC)
AMSAM-RD-PS-AM}
Redstone Arsenal, AL 00003-5898

Atlantic Research Corporation
Robert A. Camin (1 CD + 1 HC)
8945 Wellington Road
Gainesville, VA 20155-1699

CPIA
The John Hopkins University
Dr. William Hufferd (1 CD + 1 HC)
10630 Little Patuxent Parkway, Suite 202
Columbia, MD 21044-3204

Professor C. w. Smith (1 CD + 1 HC)
Virginia Polytechnic Institute and State University
ESM Dept.
Blacksburg, VA 24061-0219

Research & Development
Dr. Edmund K. S. Liu (1 CD + 1 HC)
Propulsion Division
P.O. Box 13222
Sacramento, CA 95813-6000

Ioannis Chasiotis (1 CD + 1 HC)
University of Virginia
Department of Mechanical & Aerospace Eng.
122 Engineer's Way
P.O. Box 400746
Charlottesville VA 22904-4746

Christian Meyer (1 CD + 1HC)
Columbia University
Dept of Civil Eng & Eng. Mechanics
New York, NY 10027

SEQUA
Atlantic Research Corporation
David R. Green (1 CD + 1 HC)
5945 Wellington Road
Gainesville, VA 22065

ATK Corporation
Dr. I. Lee Davis (1 CD + 1 HC)
Wasatch Operations
Box 524
Brigham City, UT 84302

Clark W. Hawk (1 CD + 1HC)
University of Alabama in Huntsville
E-26 RI Building
Huntsville, AL 35899

Daniel O. Adams (1 CD + 1 HC)
University of Utah
3116 MEB
Salt Lake City, UT 84112

Atlantic Research Corporation
Scott K. Dawley (1 CD + 1 HC)
MS 234/0
5945 Wellington Road
Gainsville, VA 20155-1699

AFOSR/IO
James M. Fillerup (1 CD _ 1 HC)
Room 732
801 N. Randolph Street
Arlington, VA 22203-1977

Ali S.. Argon (1 CD + 1 HC)
Massachusetts Institute of Technology
Room I-306
Cambridge, MA 02139

R. L. Sierakowski (1 CD + 1 HC)
Air Force Research Lab. Munitions Directorate
AFRL/MN
101 W. Eglin Parkway, Ste 105
Eglin AFB, FL 32542-6810

ATK Corporation
W. R. Hooper (1 CD + 1 HC)
Bacchus Works, M/S X11H
P.O. Box 98
Magna, UT 84044-0098

William G. Mitchell (1 CD + 1 HC)
Indian Head Division
Naval Surface Warfare Center
101 Strauss Ave.
Indian Head, MD 20640-5035